frontiers | Frontiers in Earth Science

ORIGINAL RESEARCH
published: 12 July 2022
doi: 10.3389/feart.2022.921049

New Insights Into the Paleoseismic History of the Mae Hong Son Fault, Northern Thailand

Chanista Chansom[1,2], *Sukonmeth Jitmahantakul*[1,3]*, *Lewis A. Owen*[4], *Weerachat Wiwegwin*[5] *and Punya Charusiri*[2,5]

[1]Basin Analysis and Structural Evolution Research Unit, Department of Geology, Faculty of Science, Chulalongkorn University, Bangkok, Thailand, [2]Morphology of Earth Surface and Advanced Geohazard in Southeast Asia (MESA) Research Unit, Department of Geology, Faculty of Science, Chulalongkorn University, Bangkok, Thailand, [3]M.Sc. Program in Petroleum Geoscience, Faculty of Science, Chulalongkorn University, Bangkok, Thailand, [4]Department of Marine, Earth and Atmospheric Science, North Carolina State University, Raleigh, NC, United States, [5]Department of Mineral Resources, Bangkok, Thailand

The Mae Hong Son Fault (MHSF) is a north-trending active fault in northern Thailand. The largest earthquake ever recorded in Thailand occurred in February 1975 with a magnitude of 5.6 and was associated with the southern end of the MHSF. Paleoearthquake magnitudes, recurrence intervals, and slip rates for the MHSF are evaluated using the morphological characteristics of the MHSF aided with a 12.5-m-resolution digital elevation model (DEM) and using fault trenching. Morphotectonic analysis, including studies of offset streams, linear valleys, triangular facets, and fault scarps, helps illustrate dextral fault movements within the MHSF zone. Two separated N–S trending basins, the Mae Hong Son to the north and the Mae Sariang to the south, are present along the MHSF. Between these basins, fault displacements decrease toward the Khun Yuam area. Surface rupture length investigation from fault segments in both basins indicates maximum credible earthquake magnitudes between 5.8 and 6.3. Fault trenching and road-cut studies show that nine earthquakes occurred along the MHSF over the past ~43 ka. Optically stimulated luminescence (OSL) dating help define the timing of the earthquakes to ~43, ~38, ~33, ~28, ~23, ~18, ~13, ~8, and ~3 ka. The recurrence interval of earthquakes on the Mae Hong Son Fault is ~5,000 years and the fault has a slip rate of ~0.04–0.15 mm/a.

Keywords: active fault, paleoearthquake, Mae Hong Son Fault, Mae Hong Son Basin, Mae Sariang Basin, OSL dating

OPEN ACCESS

Edited by:
Wenjun Zheng,
Sun Yat-sen University,China

Reviewed by:
Giovanni Toscani,
University of Pavia, Italy
Xiaodong Yang,
South China Sea Institute of Oceanology (CAS), China

***Correspondence:**
Sukonmeth Jitmahantakul
sukonmeth.j@chula.ac.th

Specialty section:
This article was submitted to Structural Geology and Tectonics, a section of the journal Frontiers in Earth Science

Received: *15 April 2022*
Accepted: *10 June 2022*
Published: *12 July 2022*

Citation:
Chansom C, Jitmahantakul S, Owen LA, Wiwegwin W and Charusiri P (2022) New Insights Into the Paleoseismic History of the Mae Hong Son Fault, Northern Thailand. Front. Earth Sci. 10:921049. doi: 10.3389/feart.2022.921049

1 INTRODUCTION

Thailand has experienced many M 3–6 and a few M ≥ 6 earthquakes since at least 624 BC based on historical and instrumental records (Charusiri et al., 2007; Wiwegwin et al., 2020; USGS, 2021; Thai Meteorological Department, 2022). These moderate to strong earthquakes have been detected along major fault traces in northern Thailand (**Figure 1**). Even though this region is located far away from the present-day plate boundary of Southeast Asia, the Andaman–Sumatra subduction zone (Subarya et al., 2006; McCaffrey, 2009; Roy et al., 2011), paleoseismological investigations reveal that Thailand is to some extent controlled by active indent–linked strike-slip faults due to the plate boundary (Fenton et al., 2003; Pailoplee et al., 2009; Wiwegwin et al., 2014; Pailoplee and Charusiri, 2017). The largest (Mw 6.2) instrumentally recorded earthquake in Thailand occurred on 5 May 2014, causing the greatest amount of damage in Thailand's history. The epicenter was associated with the north-trending Mae Lao Fault in Chiang Rai Province,

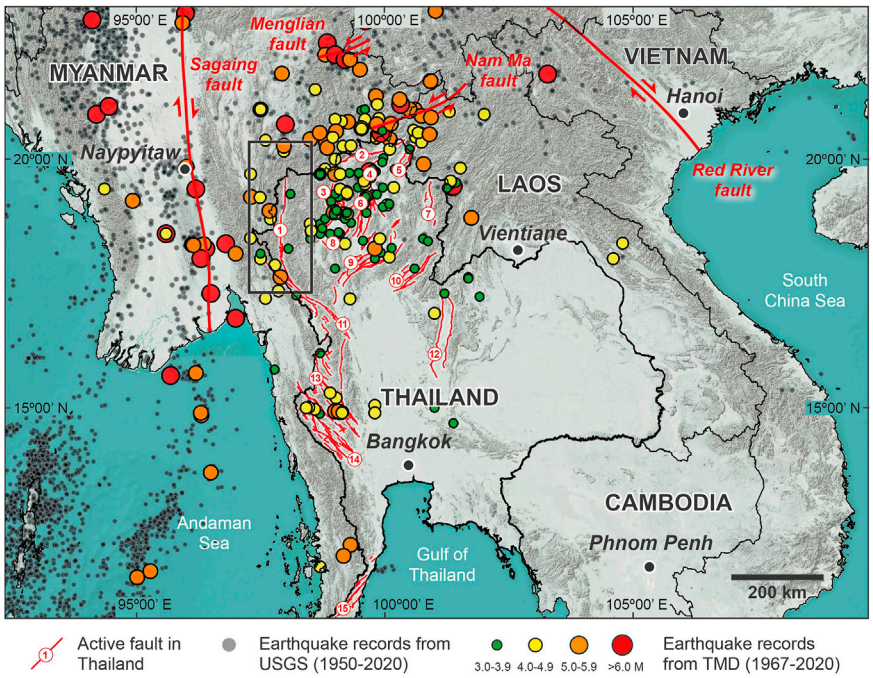

FIGURE 1 | Major active faults in Thailand and adjacent regions (modified from Department of Mineral Resources (2019) and Wang et al. (2014)) and epicentral distribution from 1967 to 2021 (USGS, 2021; Thai Meteorological Department, 2022). Fault name no. 1: Mae Hong Son Fault; 2: Mae Chan Fault; 3: Wiang Heang Fault; 4: Mae Lao Fault; 5: Mae Ing Fault; 6: Phayao Fault; 7: Pua Fault; 8: Mae Tha Fault; 9: Thoen Fault; 10: Uttaradit Fault; 11: Moei Fault; 12: Petchabun Fault; 13: Sri Sawat Fault; 14: Three Pagodas Fault; 15: Ranog Fault. The rectangle shows the location of the study area.

~27 km from Chiang Rai City. More than 50,000 people felt this earthquake, including people living in Bangkok, and more than 15,000 buildings were damaged, resulting in two deaths and 107 injuries (DDPM, 2014).

In 1975, an Mw 5.6 earthquake near the southern part of the north-trending Mae Hong Son Fault (MHSF) caused minor damage to Mae Hong Son and surrounding areas (**Figure 2**). With an intensity of VI, the earthquake was felt by people in northern and central parts of Thailand and central Myanmar (Prachaub, 1990). The MHSF is a crustal boundary fault between the Inthanon zone and the Sibumasu block (Hisada et al., 2004). The trend of the MHSF is almost parallel and close to the Sagaing Fault (~180 km to the west of Mae Hong Son Province), which is the most prominent active fault in Myanmar. Based on earthquake data and significant morphotectonic landforms, the MHSF is considered one of only a few active faults in Thailand (Charusiri et al., 2007; Department of Mineral Resources, 2019). Paleoseismic studies by Wiwegwin et al. (2014) show that there have been at least eight earthquakes within the Mae Hong Son area during the past 78 ka, with a likely earthquake recurrence interval of 10,000 years. They also suggested that there is a low probability of a large earthquake on the MHSF. The analysis of the seismic hazard by probabilistic seismic hazard analysis (PSHA) by Pailoplee and Charusiri (2016) suggested that the Mae Hong Son Province has the second-highest seismic hazard level in Thailand, with a 22% probability of exceedance (POE) of an earthquake with an intensity of VII occurring in the next 50 years.

Our study, therefore, aimed to provide a better understanding of the nature of seismicity in the Mae Hong Son area to aid in earthquake hazard assessment. We used paleoseismic studies of fault segments along the MHSF and examined the tectonic geomorphology using high-resolution digital elevation models, Landsat-7 images, and satellite images available on Google Earth. In addition, we defined the fault slip rate, date past earthquakes, and determine earthquake recurrence intervals along the MHSF. The study area covers ~25,500 km^2 and is bounded by latitude 17°38′N–19°48′N and longitude 97°20′E–98°39′E in Mae Hong Son Province. Fault trenching and tectonic geomorphology were carried out across the three selected fault segments along the MHSF, which we name Ban Yod, Khun Yuam, and Mae Tha Lu. The Ban Yod fault segment is a ~4.2-km-long NNE-trending right-lateral strike-slip fault, at the northern end of the MHSF (**Figure 3**). The Khun Yuam fault segment is in the central part of the MHSF zone and is a ~3.5-km-long N- to NNE-trending right-lateral strike-slip fault that cuts across Khun Yuam District (**Figures 2**, **3**). The Mae Tha Lu fault segment at the southern end of the MHSF is a ~8.8-km-long N- to NNW-trending right-lateral strike-slip fault (**Figure 4**). We, then, compared our paleoseismic findings with previous studies.

2 NEOTECTONIC SETTING AND PRESENT-DAY SEISMICITY

Seismicity in the Myanmar–Laos–Northern Thailand region is associated with Indian–Eurasian continental–continental collision (Peltzer and Tapponnier, 1988; Wang et al., 2014). A NE-to NNW-trending strike-slip fault network is dominant and has developed

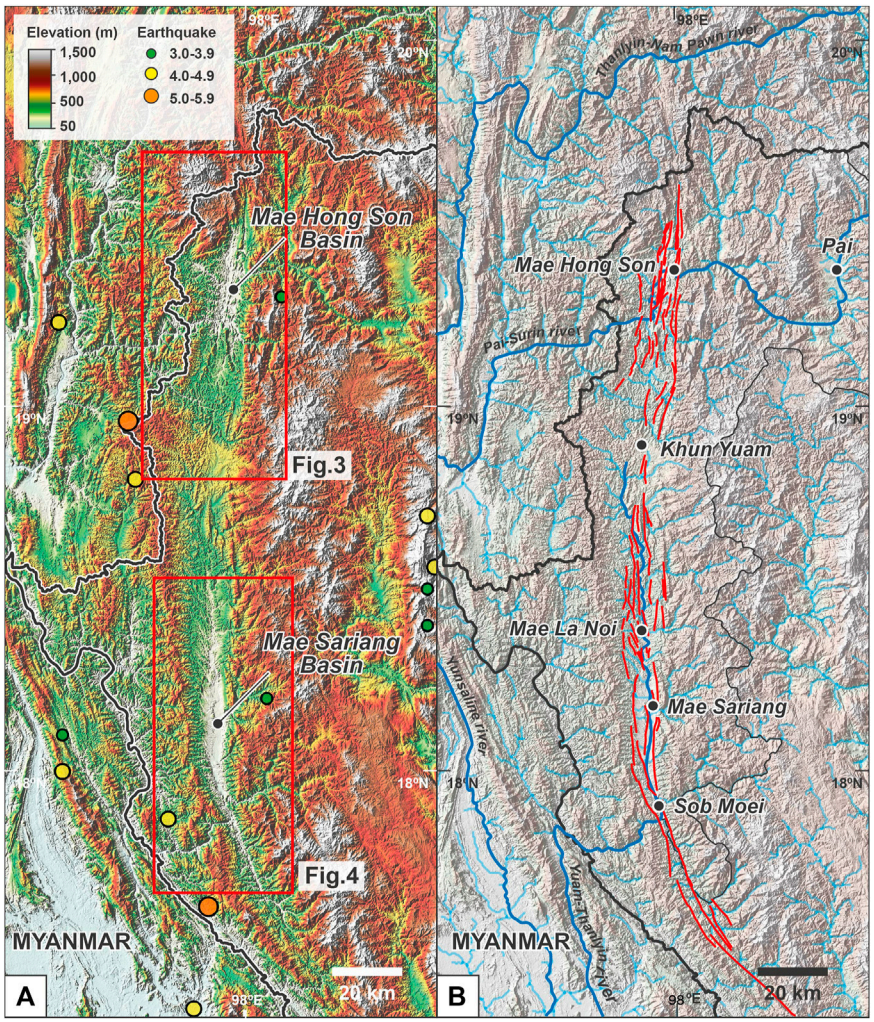

FIGURE 2 | Study area shows: **(A)** enhanced ALOS DEM data highlighting the Mae Hong Son Basin in the north and the Mae Sariang Basin in the south of the Mae Hong Son Province; and **(B)** hillshade ALOS DEM and stream maps highlight the north trending fault segments throughout Mae Hong Son Province. The red rectangles in part **(A)** highlight the geomorphic study areas shown in other figures.

since the Late Cretaceous (Morley, 2004). Some of these fault trends strongly followed pre-collision fabrics within the West Burma and Sibumasu terranes (Morley et al., 2007; Searle and Morley, 2011). As India moved northward into Asia, several of the major faults, such as the Red River, Moei (also known as Mae Ping), and Three Pagodas faults (**Figure 1**), have rotated clockwise and moved laterally. A regional reversal of slip from left to right lateral on these faults is placed around the Late Oligocene (Allen et al., 1984; Lacassin et al., 1997; Lacassin et al., 1998).

Historical and instrumental recorded seismicity shows that at least 20 destructive earthquakes with M > 6 have occurred in this region (Ekström et al., 2012; Shi et al., 2018). Most earthquakes are clustered along the sinistral and dextral strike-slip faults between the Sagaing (bounds on the west) and the Red River (bounds on the east) faults (**Figure 1**). Recent significant earthquakes on these faults include the 1988 Mw 7.0 Lancang–Gengma earthquake at the north-western end of the Lancang Fault in south China (Chen and Wu, 1989), the 1995 Mw 6.8 Menglian earthquake at the southern of the Menglian Fault in eastern Myanmar (Ji et al., 2017), the 2011 Mw 6.8 Tarlay earthquake at the western end of the Nam Ma Fault in eastern Myanmar (Tun et al., 2014), and the 2014 Mw 6.1 Mae Lao earthquake along the Mae Lao Fault in northern Thailand (Pananont et al., 2017). In addition, small and shallow earthquakes in the Myanmar–Laos–Northern Thailand region demonstrate widespread deformation across the fault systems between the Sagaing and the Red River faults, suggesting that these faults are active today.

3 MORPHOTECTONIC LANDFORM INTERPRETATION

High-resolution terrain corrected ALOS PALSAR dataset 2007 with a pixel size of 12.5 m, Landsat-7 images satellite from

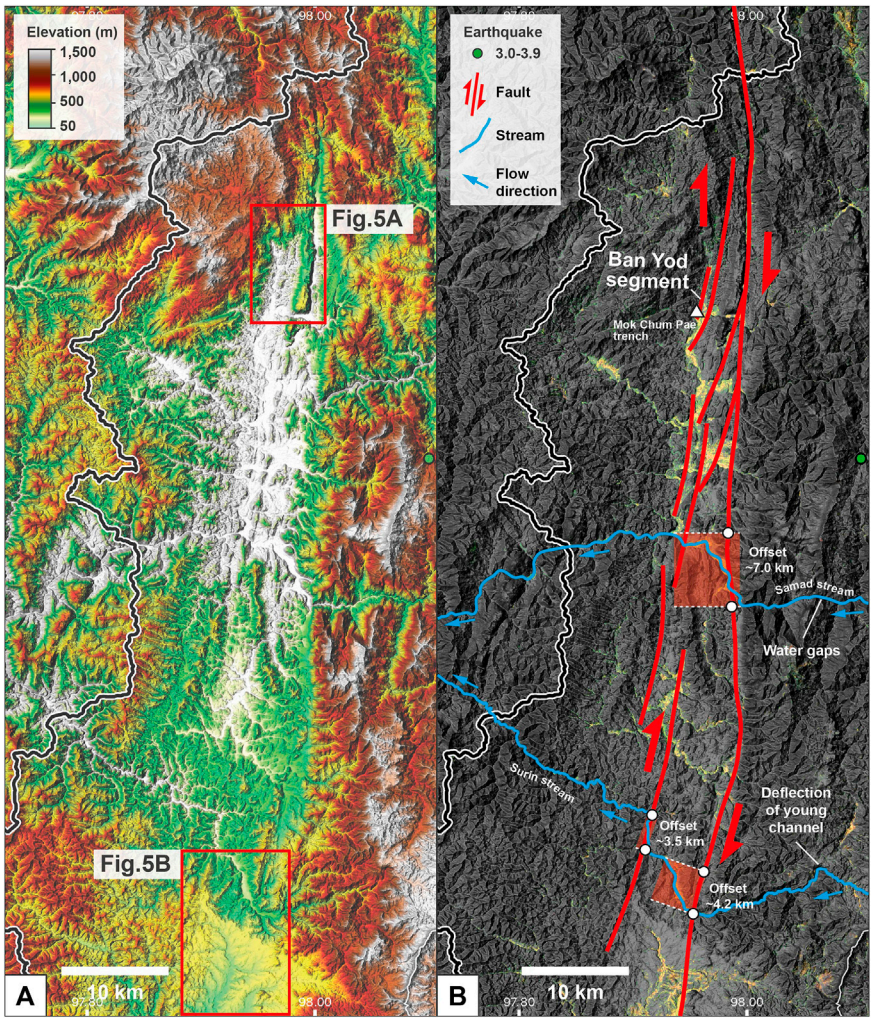

FIGURE 3 | Mae Hong Son Basin on the north side of Mae Hong Son Province is shown as an **(A)** enhanced ALOS DEM, and **(B)** detailed interpretation at the Samad stream displays offset stream with maximum offset of ~7.0 km suggesting the right-lateral strike-slip fault movement and at the Surin stream shows offset stream of ~3.5 and ~4.2 km (maximum offset ~7.7 km) also suggesting the right lateral strike-slip fault movement. Locations are shown in **Figure 2A**.

National Aeronautics and Space Administration (NASA), and most recent high-resolution images available in Google Earth date to 2021 were analyzed for identifying the morphotectonic landforms implying the possible active fault segments in the MHSF (**Figure 2**). Triangular facets, fault scarps, linear valleys, hot springs, offset streams, and shutter ridges were mapped.

Several offset streams in the study area occur along the MHSF (**Figures 3**, **4**). These include the Samad stream at the Ban Pha Bong segment, Surin stream at the Ban Mae Surin segment, and Mae Han and Mae Salab streams in the Mae Sariang Basin with maximum displacements of 7.0, 7.7, 4.0, and 4.6 km, respectively. The lengths of the shuttle ridges in the study area range from 150 to 300 m. Good examples are Ban Khun Yuam (150-m-long) in the middle part of the MHSF (**Figure 5B**) and Ban Mae Tha Lu (250-m-long) in the southern part of the MHSF (**Figure 5C**). Linear valleys are also present along the MHSF, such as at Ban Yod (5-m-long) in the north (**Figure 5A**) and Khun Yuam in the middle stretches of the MHSF (**Figure 5B**). Triangular facets have height ranges from 1 to 5 m and their base varies from 2 to 10 m. Several triangular facets are present along the MHSF at Ban Yod, Khun Yuam, and Ban Mae Tha Lu (**Figures 5A–C**). Several fault scarps are present along the MHSF, particularly at Ban Yod and Khun Yuam fault segments.

4 PALEOEARTHQUAKE STUDY

4.1 Trench Excavations and Stratigraphy

4.1.1 Ban Yod Trench

The Ban Yod Fault trench is located (19°26′29″N and 97°57′41″E; **Figure 5A**) within the Ban Yod segment where small offset streams and fault scarps were observed. The trench was 19-m-long, 3-m-wide, and 3-m-deep. Seven depositional units (A–G) were exposed in both sidewalls (**Figure 6**; **Table 1**).

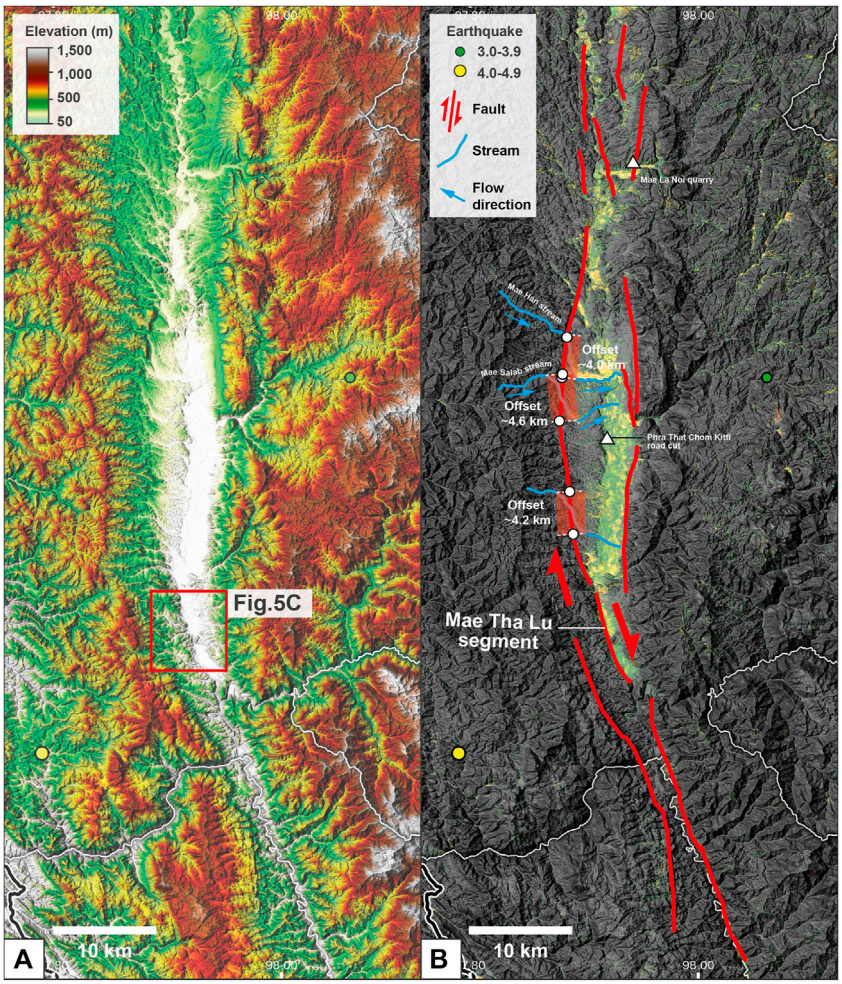

FIGURE 4 | Mae Sariang Basin on the south of the Mae Hong Son Province shows **(A)** enhanced ALOS DEM, and **(B)** detailed interpretation at the Mae Han stream displays offset stream with maximum offset of ~4.0 km suggesting the right lateral strike-slip fault movement and at the Mae Salab stream shows the offset stream of ~4.6 km suggesting the dextral movement. Locations are shown in **Figure 2A**.

Unit A is the oldest unit and is a 0.5–1.25-m-thick colluvium deposit composed of brownish-gray gravel with largely moderately sorted clast-supported subangular to rounded pebbles to cobbles with a matrix of fine sand, silt, and clay. The clasts are mainly sandstone, shale, and quartz. Unit B is a ~0.6-m-thick colluvial deposit consisting of moderately sorted clast-supported subangular to subrounded boulders, pebbles, sand, silt, and clay, mainly of sandstone and shale. Unit C is a ~0.1-m-thick fluvio-lacustrine deposit that contains a few gravels within a dark gray clayey silt matrix. The gravels are usually subangular sandstone fragments. This unit contains a lot of charcoal fragments. Unit D (av. 0.60-m-thick) is an alluvial unit with light gray clay with a fine sand layer. This unit shows laminations.

Unit E is a ~0.40-m-thick fluvial deposit of clast-supported gravel, sand, silt, and clay. Most clasts are subangular and composed mainly of sandstone, shale, and quartz. Unit F is a ~0.5-m-thick colluvial deposit within a channel and is composed of clast-supported subrounded to rounded gravel unit mainly consisting of sandstone, shale, and quartz. At least three graded bedding are present, and the upper part of this unit contains dark clay. The succession is capped with dark topsoil which is unit G that has some sand and clay lens. Units A and C are displaced by an east-dipping dip-slip fault. Units E, F, G, and H were deposited and covered by unit I and topsoil Unit D.

4.1.2 Khun Yuam Trench

The Khun Yuam Fault trench is located at a frontal foothill (18°48′43″N and 97°56′33″E; **Figure 5B**), near Khun Yuam District. The 18-m-long, 3-m-wide, and 3.5-m-deep trench exposed 12 depositional units (A-L) in both of its walls (**Figure 7**; **Table 1**).

Unit A is a ~0.4-m-thick alluvial deposit with light brownish gray, mainly clay with a few gravels. Unit B is a ~0.2-m-thick alluvial/colluvial deposit of gravel, sand, and clay. The gravel is pebble size (1.5 cm). Unit C is a ~0.1-m-thick colluvial/alluvial deposit that contains light brown to yellowish-brown sand, silt, and clay, and some gray to purple. The sediments in this unit are

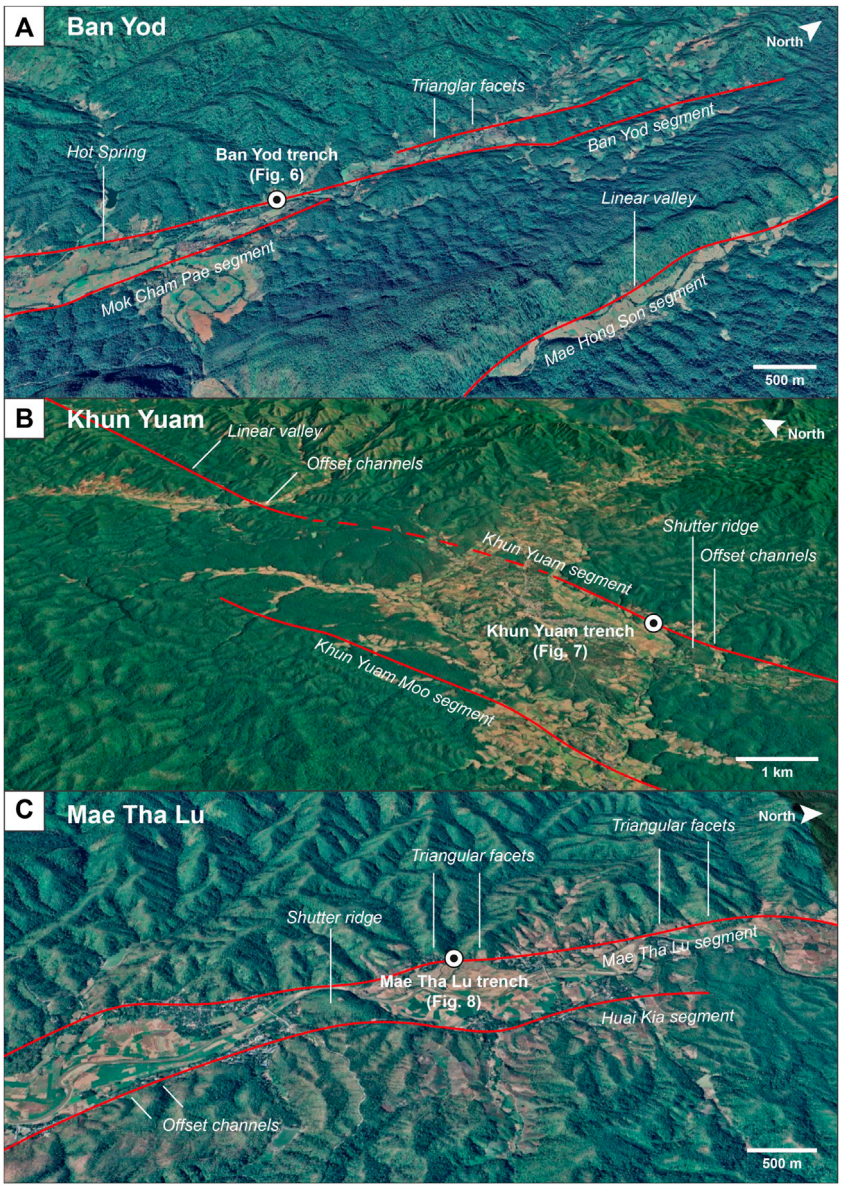

FIGURE 5 | Google Earth images show the location of the fault trenches and detailed tectonic geomorphic evidence at **(A)** the Ban Yod, **(B)** Khun Yuam **(B)**, and **(C)** Mae Tha Lu.

mainly clay with sand and sand lens. Unit D is a ~0.5-m-thick colluvial deposit that is composed of moderate to poorly sorted gravel, sand, silt, and clay. The clasts are subangular to subrounded pebbles to boulders.

Unit E is a ~0.5-m-thick fluvial channel deposit composed of sand, silt, and clay. The grain size is generally pebble of quartz and sandstone. At least three graded beds are present. Unit F is a ~0.2-m-thick alluvial deposit that contains orangish-brown sand, silt, and clay. Unit G is a ~0.6-m-thick alluvial channel deposit that contains yellowish-brown sand, silt, and clay with some gravel. The gravel size ranges from pebble to cobble. The lamination and chaotic structure could be found in the unit. Unit H is a ~0.2-m-thick alluvial channel deposit that contains dark brown to brownish-gray sand and gravel. The gravel size ranges from pebble to cobble and the gravel shape is subangular to subrounded. The sediments in this unit are moderately well sorted.

Unit I is a ~0.25-m-thick alluvial that contains yellowish-brown silt, sand, and gravel. The sediments in this unit are mainly silt and sand with scattered gravel. The gravel size ranges from pebble to cobble and the gravel shape is angular to subrounded. The sediments in this unit are moderately well sorted. Unit J is a ~0.2-m-thick colluvial deposit that is composed of dark brown gravel, sand, silt, and clay. The gravel is matrix-supported and

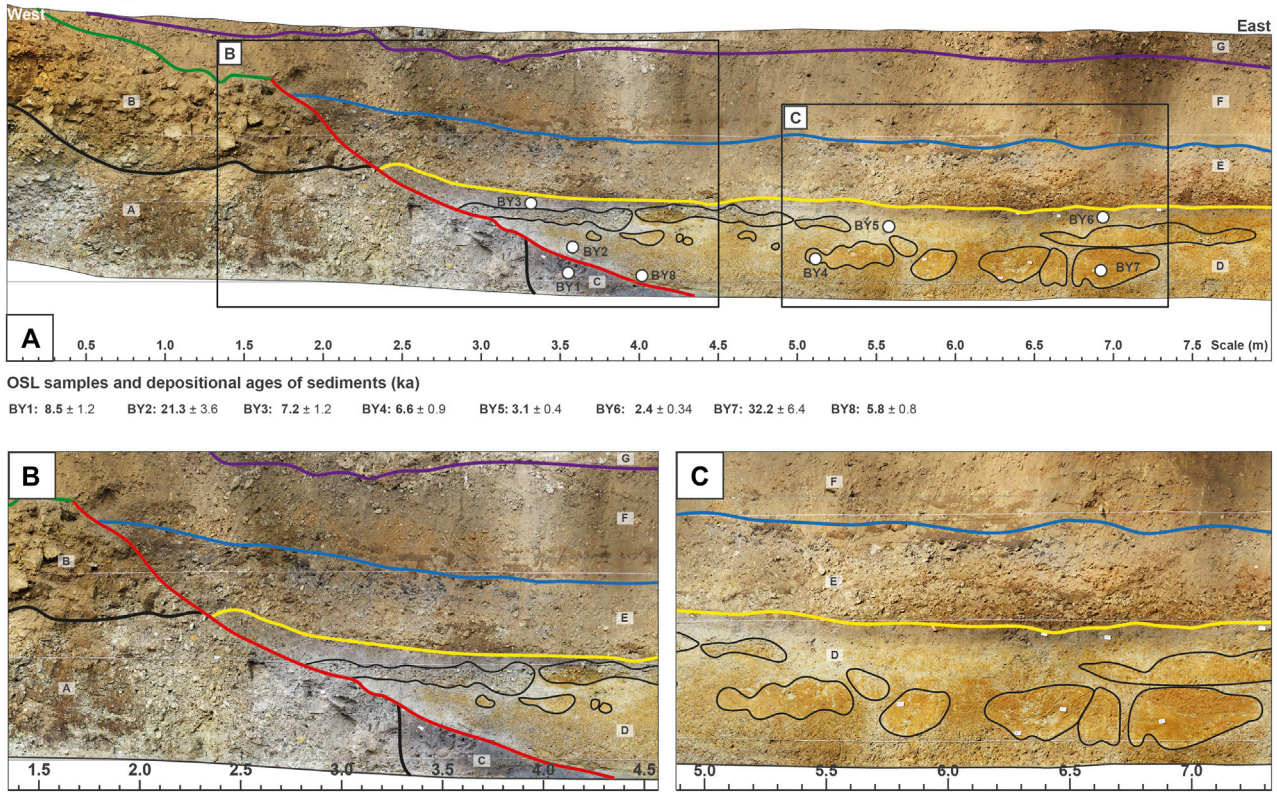

FIGURE 6 | Sections and wall logs for the north wall Ban Yod trench showing sediments, stratigraphy, fault orientation, sample locations for dating, and OSL ages (in ka) of sediment layers. The trench location is shown in **Figure 5A**. **(A)** North wall of Ban Yod trench. **(B)** View showingdiscontinuity of sediment layer and fault traces (red line) were observed on the wall. **(C)** View showing discontinuity of sediment layer, suggesting possibly a soft-sediment deformation due to earthquake stress.

mainly composed of poorly to moderately sorted angular to subrounded pebbles to cobbles up to 12 cm in diameter, mainly sandstone, shale, quartz, and granite.

Unit K is a ~0.35-m-thick alluvial deposit clast of weathered rock of sand and gravel, matrix: fine sand, clay. The succession is capped with soil that has laminated fine to very coarse sand. Sediment structures in unit F and unit G are soft-sediment deformation, they are mostly ball-and-pillow structures from unconsolidated sediment with low shear resistance because of tectonic or sedimentary processes (Allen, 1982). The soft-sediment deformation structures in the Khun Yuam trench are interpreted to be produced by seismic activity. Units A, B, C, and D are displaced by an oblique strike-slip fault (**Figure 7**).

4.1.3 Mae Tha Lu Trench

The Mae Tha Lu Fault trench is located (17°58′45″N and 97°55′34″E; **Figure 5C**) at a frontal foothill, near Mae Sariang District. The 14-m-long, 3-m-wide, and 3.5-m-deep trench exposed basement rock and nine depositional units (A–H) and topsoil in both walls of the trench (**Figure 8**; **Table 1**).

Unit A is a ~1.5-m-thick colluvial deposit that contains reddish-brown gravel and sand. These clasts are clast-supported and are subangular to subrounded sandstone and shale. The sediment ranges from boulders to cobbles with fining upward succession. Unit B is a ~0.4-m-thick colluvial deposit that contains clay with gravel, almost fine grain, and gravel can be found in the west of the trench, matrix-supported, lateritic texture, more Fe and Mn concretion (black spot). Unit C is a ~0.25-m-thick colluvial deposit consisting of gravel, sand, silt, and gravel. The gravels ranging in size from pebble to cobble are fine-grained sandstone and shale, well-sorted to moderate-sorted (with more clay in the lower part). Unit D is a ~0.5-m-thick alluvial deposit composed of clay, silt with Fe or Mn concretion, and little gravel. Gravels mostly are quartz, with a reddish-brown lateritic texture.

Unit E is a ~0.3-m-thick alluvial deposit consisting mainly of sand and clay, with a few gravels present. Unit F is a ~0.6-m-thick alluvial deposit composed of matrix-supported, angular to subrounded gravel, sand, silt, and clay. Unit G is a ~0.5-m-thick colluvial deposit composed of, matrix-supported, angular to subrounded clasts are quartz and sandstone. Unit H is a ~0.2-m-thick alluvial deposit composed of dark brown sand, silt, and clay. The succession is capped with a ~0.3-m-thick dark brown soil unit, composed mainly of sand, silt, and clay with some roots. Unit A is a colluvial wedge associated with a 70°-dipping and ENE (062°) trending oblique strike-slip fault, with some gravels near

TABLE 1 | Description of stratigraphic units in trenches at Ban Yod, Khun Yuam, and Mae Tha Lu, as presented in **Figures 6–8**.

Unit	Description
Ban Yod trench	
G	Dark sandstone and clay lens; topsoil
F	Dark brown, clast-supported sandy gravel. Clasts are subrounded to rounded. The upper part of this unit contains dark clay; fluvial deposit
E	Brown, clast-supported sandy gravel. Most clasts are subangular; fluvial deposit
D	Light gray, matrix-supported silty sand, lamination, gravel lens, dark clay layer on the top, fining upward; alluvial deposit
C	Dark gray, matrix-supported clayey silt with scattered gravels. The gravels are subangular sandstone fragments; fluvio-lacustrine deposit
B	Brownish-gray, clast-supported with pebbly to boulder gravel. Clasts are mainly of subangular to subrounded sandstone and shale, moderately sorted (gravel size); colluvial deposit
A	Brownish-gray, clast-supported with pebbly to cobbly gravel. Most clasts are subangular to rounded with moderately sorted, fining upward; colluvial deposit
Khun Yuam trench	
L	Dark brown and gray, matrix-supported with silty sand, found roots; topsoil
K	Light brown, matrix-supported clayey sand with scattered weather rocks and gravel; alluvial deposit
J	Brownish-gray, matric-supported gravely sand with scattered pebbly to cobbly gravel. Most clasts are angular to subangular of shale, quartz and granite, poorly sorted; colluvial deposit
I	Yellowish-brown, matrix-supported silty sand with scattered pebbly gravel. Most clasts are angular to subrounded, moderately sorted; alluvial deposit
H	Dark brown to brownish-gray, clast-supported sandy gravel. Most clasts are subangular to subrounded. The gravel size ranges from pebble to cobble, moderately sorted; alluvial deposit (channel sediment)
G	Yellowish-brown, matrix-supported sandy silt with scattered pebbly to cobbly gravels, lamination and chaotic structure; alluvial deposit
F	Light brown, matrix-supported clayey sand with scattered pebbly gravel; alluvial deposit
E	Light brown to dark brown, sandy silt with pebbly gravel. Graded bedding at least three sequences; fluvial deposit (channel sediment)
D	Yellowish-brown, gravely sand with scattered pebbly to boulderly gravel. Most clasts are subangular to subrounded, moderate to poorly sorted; colluvial deposit
C	Yellowish-brown with some gray to purple, silty clay with sand lens; alluvial deposit
B	Light brown, matrix-supported gravely sand with scattered gravel. Most clasts are pebble, wedge shape; alluvial deposit
A	Light brownish-gray, silty clay with scattered gravel; alluvial deposit
Mae Tha Lu trench	
I	Dark brown, mainly sand, silt, and clay with some roots; topsoil
H	Dark brown, fine-grained sand, silt, and clay with scattered pebbles; alluvial deposit
G	Brown, matrix-supported with silt and sand. Clasts are angular to subrounded. Some roots can be observed here; colluvial deposit
F	Dark reddish-brown, matrix-supported sand, silt, and clay with scattered pebbles. Clasts are angular to subrounded; alluvial deposit
E	Reddish-brown, matrix-supported sand and silt with scattered pebbles; alluvial deposit
D	Reddish-brown, matrix-supported silty sand with scattered pebbles. Fe and Mn concretion with lateritic texture; alluvial deposit
C	Reddish-brown, clast-supported pebbly to cobbly gravel and sandy gravel, well- to moderate-sorted; colluvial deposit
B	Brown, matrix-supported silty sand with scattered pebbles. Fe and Mn concretion with lateritic texture, continually deposit from A3; colluvial deposit
A	Reddish-brown, clast supported pebbly and cobbly gravel with subangular to subrounded gravels. Boulders of conglomerate with bedding of gravel; colluvial deposit

the fault plane aligned at a high angle to bedding. Surface morphology such as triangular facets that are commonly found in this area supports dominant normal faulting.

4.2 Dating Results and Paleoearthquake Events

All 22 OSL samples were collected from sandy clay and silty sand units from the Ban Yod, Khun Yuam, and Mae Tha Lu trenches (**Table 2**). The samples were analyzed in the Geochronology Laboratories at the University of Cincinnati. **Table 2** provides radioisotope, water content, cosmic dose rate, DR and DE values, and OSL ages of each sample, with explanations of the methods used to calculate dose rates and age calculation uncertainties. Dose rate calculations follow the details highlighted in the table's footnotes and are confirmed using the Dose Rate and Age Calculator (DRAC) of Durcan et al. (2015). The DR for all samples has

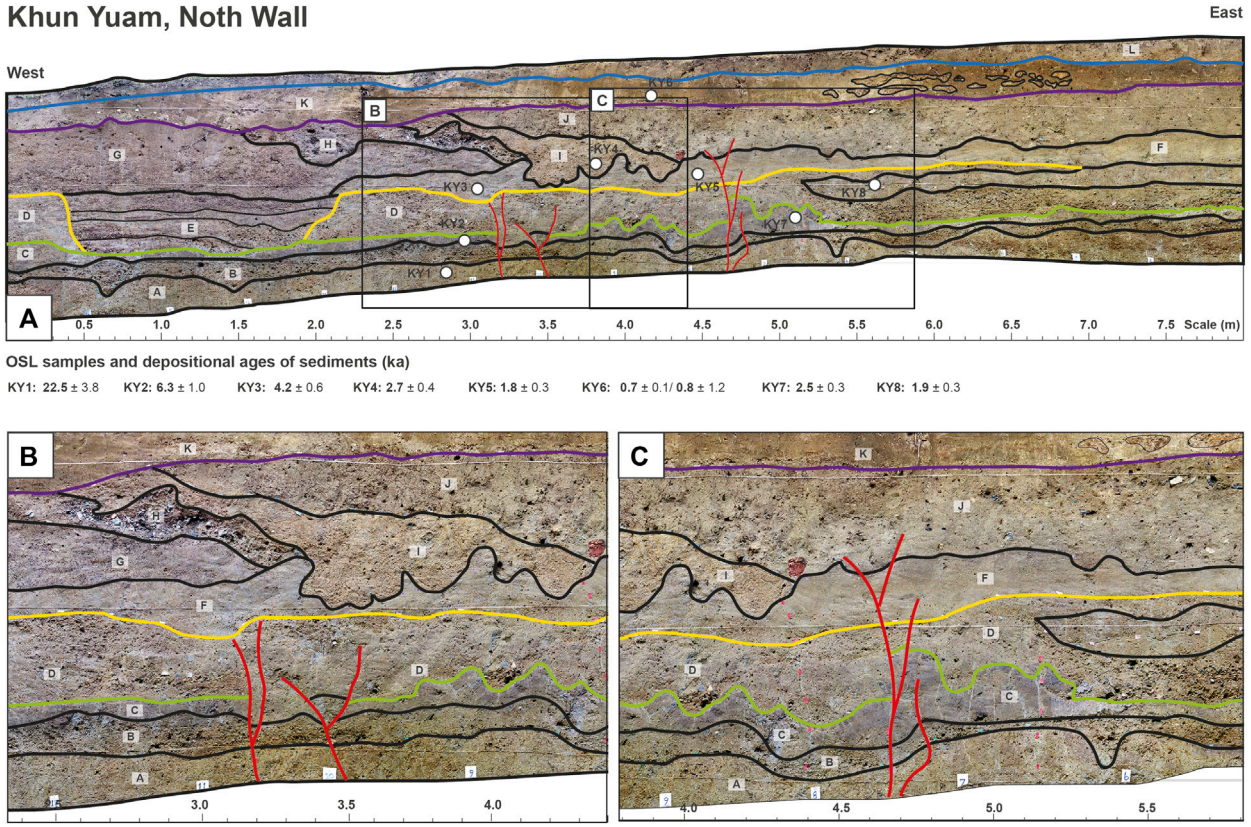

FIGURE 7 | Sections and wall logs on the north wall at Khun Yuam trench showing sediment stratigraphy, fault orientation, sample locations for dating, and OSL ages (in ka) of sediment layers. The trench location is shown in **Figure 5B**. **(A)** North wall of Khun Yuam trench **(B)** and **(C)** closed-up photographs showing discontinuity of sediment layer and fault traces (red line) were observed in the wall.

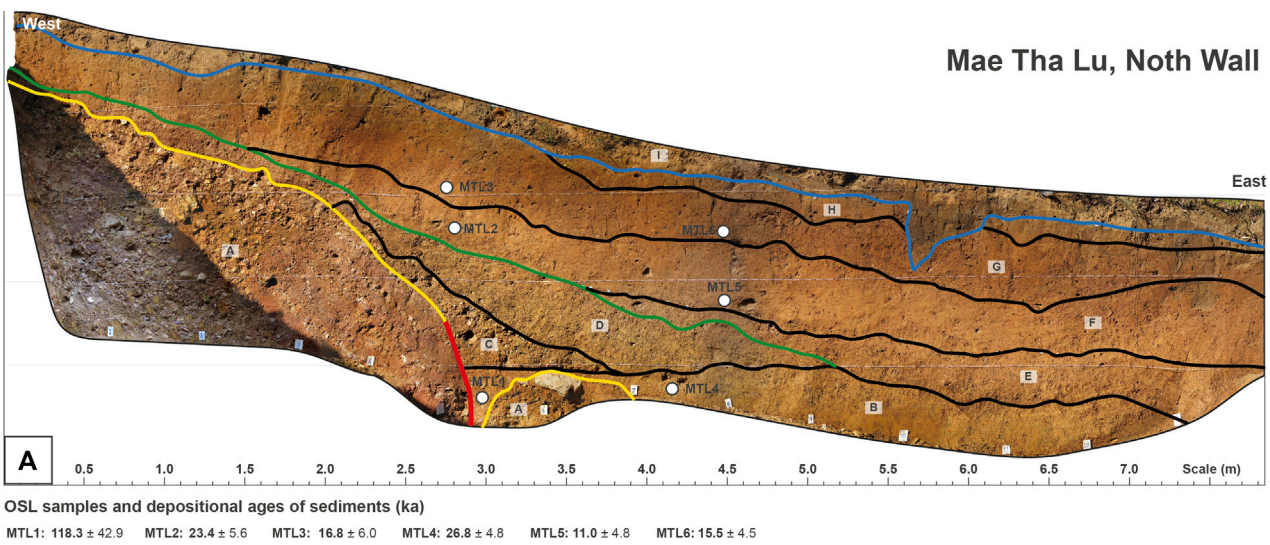

FIGURE 8 | Paleoearthquake trench section and wall log section on the north wall at Mae Tha Lu trench showing sediment stratigraphy, fault orientation, sample locations for dating, and OSL ages (in ka) of sediment layers. The trench location is shown in **Figure 5C**.

TABLE 2 | OSL dating results of extracted sediments from the study area, Mae Hon Son Province, northern Thailand, containing radioisotope concentrations, moisture content total dose rate, equivalent dose estimates, and absolute ages.

Trench	Sample name	Unit	U[a] (ppm)	Th[a] (ppm)	K[a] (%)	Rb[a] (ppm)	Depth (m)	Latitude (°S)	Longitude (°W)	Altitude (m asl)	Cosmic dose rate[b,c] (Gy/ka)	Total equivalent dose rate[b,c,d] (Gy/ka)	Number of aliquots that past all test and uses in age calculations[e]	Dispersion (%)	DE arithmetic mean[f] (Gy)	Arithmetic mean age[j] (ka)	DE weighted mean[h] (Gy)	Weighted mean age[j] (ka)
BY	BY1	C	1.43	9.08	0.91	122.70	3.0	19.4416	97.9613	236	0.14±0.02	1.47±0.10	6	7	14.52±0.49	9.9±4.8	12.5±0.13	8.5±1.2
BY	BY2	D	1.53	7.73	0.68	107.50	2.5	19.4416	97.9613	236	0.15±0.02	1.29±0.09	6	8	32.19±1.25	25±14.2	27.48±0.32	21.3±3.6
BY	BY3	D	1.05	4.25	0.32	96.10	2.0	19.4416	97.9613	236	0.16±0.02	0.68±0.04	6	4	5.62±0.12	8.2±3.1	4.88±0.05	7.2±1.2
BY	BY4	D	0.70	8.52	1.45	75.30	2.5	19.4416	97.9613	236	0.15±0.02	1.63±0.12	24	18	12.82±0.48	7.9±4.0	10.69±0.11	6.6±0.9
BY	BY5	D	0.74	8.27	1.36	81.80	2.5	19.4416	97.9613	236	0.15±0.02	1.67±0.13	15	13	6.08±0.21	3.7±1.7	5.11±0.06	3.1±0.4
BY	BY6	D	0.18	7.30	1.39	90.80	2.3	19.4416	97.9613	236	0.15±0.02	1.43±0.11	17	15	4.03±0.17	2.8±1.6	3.37±0.03	2.4±0.3
BY	BY7	D	1.35	5.97	0.49	75.30	2.3	19.4416	97.9613	236	0.15±0.02	0.86±0.05	6	3	31.73±0.58	37.1±11.9	27.51±0.31	32.2±6.4
BY	BY8	D	0.50	8.31	1.40	102.30	2.8	19.4416	97.9613	236	0.14±0.02	1.55±0.12	24	11	10.53±0.26	6.8±2.3	9.02±0.09	5.8±0.8
KY	KY1	A	7.14	32.12	3.46	196.90	3.0	18.8120	97.9426	547	0.15±0.02	4.24±0.27	8	7	111.58±3.21	26.3±11.9	95.41±1.03	22.5±3.8
KY	KY2	C	6.73	27.98	2.08	139.40	2.5	18.8120	97.9426	547	0.16±0.02	3.37±0.21	6	7	24.80±0.79	7.3±3.7	21.38±0.21	6.3±1.0
KY	KY3	F	6.25	30.20	2.02	130.90	1.8	18.8120	97.9426	547	0.17±0.02	3.44±0.22	7	9	16.99±0.69	4.9±3.2	14.51±0.13	4.2±0.6
KY	KY4	I	5.52	20.97	3.52	193.20	1.5	18.8120	97.9426	547	0.18±0.02	4.17±30	6	7	13.18±0.42	3.2±1.4	11.37±0.11	2.7±0.4
KY	KY5	F	3.59	41.63	1.53	121.90	1.8	18.8120	97.9426	547	0.17±0.02	3.47±0.24	21	17	7.34±0.33	2.1±1.4	6.10±0.06	1.8±0.3
KY	KY6	K	3.23	38.07	4.44	183.30	0.5	18.8120	97.9426	547	0.21±0.02	4.78±0.33	20	45	5.16±0.76	1.1±2.3	3.41±0.04	0.7±0.1/ 0.8±1.2[i]
KY	KY7	C	3.25	40.78	1.95	129.40	2.5	18.8120	97.9426	547	0.16±0.02	3.68±0.26	23	14	11.15±0.37	3.0±1.5	9.36±0.08	2.5±0.3
KY	KY8	D	3.10	30.71	1.30	121.10	2.0	18.8120	97.9426	547	0.17±0.02	2.79±0.19	21	8	6.32±0.14	2.3±0.7	5.43±0.05	1.9±0.3
MTL	MTL1	B	1.24	9.31	1.73	26.81	2.8	17.9793	97.9176	178	0.14±0.02	1.98±0.15	6	7	267.46±12.01	135.3±80.0	233.98±6.43	118.3±42.9
MTL	MTL2	F	1.80	15.55	1.93	25.61	1.3	17.9793	97.9176	178	0.17±0.02	2.93±0.24	6	3	78.93±1.86	26.9±7.8	68.63±1.34	23.4±5.6
MTL	MTL3	G	1.99	13.88	1.54	26.19	1.0	17.9793	97.9176	178	0.18±0.02	2.22±0.16	6	8	42.74±1.96	19.3±12.4	37.30±0.94	16.8±6.0
MTL	MTL4	B	1.09	19.03	3.11	25.37	2.5	17.9793	97.9176	178	0.15±0.02	2.97±0.22	20	9	92.86±2.27	31.2±10.4	79.70±1.05	26.8±4.8
MTL	MTL5	F	1.48	18.41	2.76	25.86	1.1	17.9793	97.9176	178	0.18±0.02	3.88±0.34	7	8	50.92±2.61	13.1±7.7	42.67±1.63	11.0±4.8
MTL	MTL6	G	1.80	13.84	1.44	26.45	1.4	17.9793	97.9176	178	0.17±0.02	2.23±0.16	6	3	39.63±1.09	17.8±6.6	34.41±0.74	15.5±4.5

[a]Elemental concentrations from gamma-ray spectrometry of whole sediment measured at Kasetsart University, Bangkok, Thailand.

[b]Estimated fractional day water content for whole sediment is taken as 10% and with an uncertainty of ± 5%.

[c]Estimated contribution to dose-rate from cosmic rays calculated according to Prescott and Hutton (1994). Uncertainty taken as ±10%.

[d]Total dose-rate from beta, gamma, and cosmic components. Cosmic dose rate was determined using Prescott and Hutton (1994). Beta attenuation factors for U, Th and K compositions incorporating grain size factors from Mejdahl (1979). Beta attenuation factor for Rb is taken as 0.75 (cf. Adamiec and Aitken, 1998). Factors utilized to convert elemental concentrations to beta and gamma dose-rates from Adamiec and Aitken, 1998) and beta and gamma components attenuated for moisture content. Dose rates calculation was confirmed using the Dose Rate and Age Calculator (DRAC) of Duncan et al. (2015).

[e]Number of replicated equivalent dose (D_E) estimates used to calculate D_E. These are based on recuperation error of < 10%. The number in the parentheses is the total measurements made including failed runs with unusable data. The number in square parentheses is the percentage of aliquots used for minimum age 2-mixing model.

[f]Average equivalent dose (D_E) determined from replicated single-aliquot regenerative-dose (SAR; Murray and Wintle, 2000) runs. The uncertainty is the standard error and includes an uncertainty from beta source estimated of ±2.5%.

[h]Weighted average equivalent dose (D_E) determined from replicated single-aliquot regenerative-dose (SAR; Murray and Wintle, 2000) runs. The uncertainty is the standard error and includes an uncertainty from beta source estimated of ±2.5%.

[i]Age based on minimum population in 2-mixing model using the program of Vermeesch (2009). 0.8 ± 1.2 age is based on minimal age from two mixing model.

[j]Uncertainty incorporate all random and systematic errors, including dose rates errors and uncertainty for the D_E.

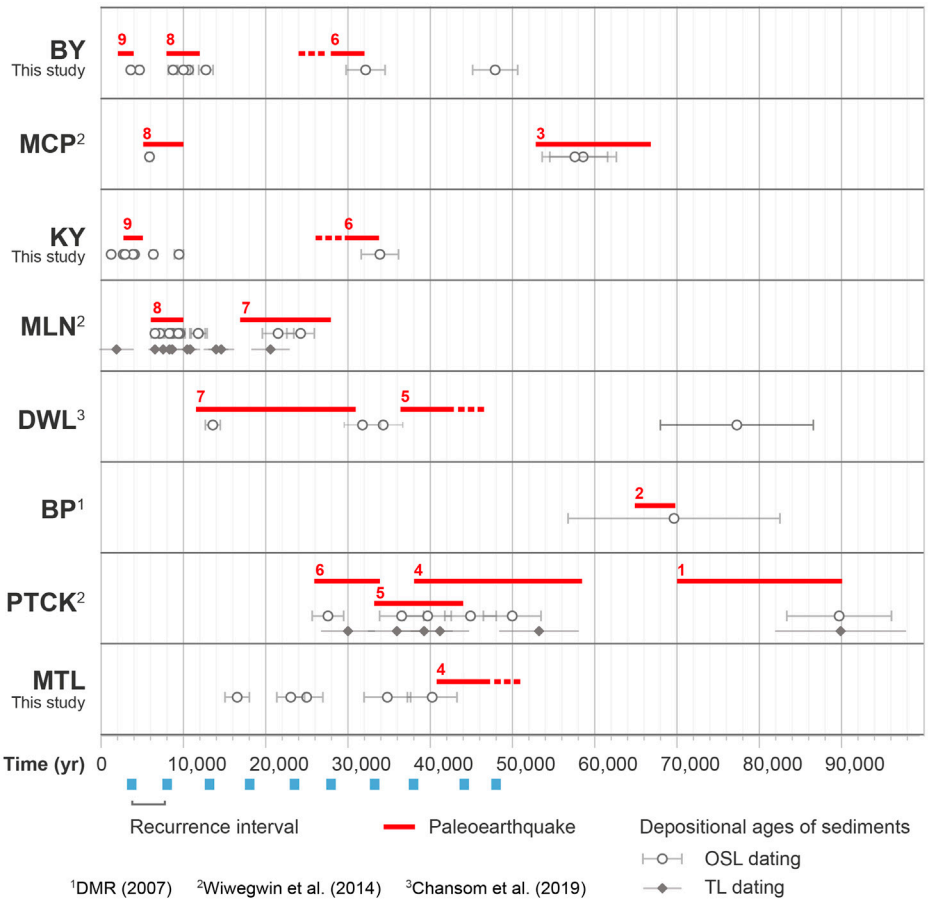

FIGURE 9 | Diagram shows the depositional ages of young sediments in the trenches from the OSL ages (in years BP) and interpreted paleoearthquake events in individual trenches, MHSF. Fault segments: Ban Yod (BY), Mork Cham Pae (MCP), Khun Yuam (KY), Mae La Noi (MLN), Doi Wiang Luang (DWL), Ban Pae (BP), Phra Tat Chom Kitti (PTCK), Mae Tha Lu (MTL).

TABLE 3 | Rates of right-lateral strike-slip faulting along the Mae Hong Son Fault.

Lateral slip rate: Ban Yod segment					
Measure	**Mean**	**Mode**	**Median**	**68.27% Interval**	**95.45% Interval**
Offset (m)	4	4	4	+0.1/–0.1	+0.2/–0.2
Age (ka)	3	3	3	+1/–1	+0.2/–0.2
Slip rate (mm/yr)	1.5	1.1	1.3	+0.7/–0.3	+2.4/–0.5
Lateral slip rate: Mae Tha Lu segment					
Offset (m)	6.8	10	6.6	+3.3/–2.6	+3.4/–2.8
Age (ka)	48	48	48.1	+10/–10.1	+20/–20
Slip rate (mm/yr)	0.1	0.1	0.1	+0.1/–0.1	+0.2/–0.1

a value that varies from 0.64 to 4.78 Gy/ka within the normal range for terrestrial sediments. The water contents of samples are between 16 and 69%.

The spread of DE for the most samples with low dispersion (< 20%), we use the weighted mean value for the DE values (**Table 2**). However, there is one sample (sample name: KY6) where the spread of DE was relatively large for this sample (dispersion> 20%), suggesting possible partial bleaching. This can result in an overestimate of age. For this sample, we assumed a 2-mixing model using the Radial Plotter (Vermeesch, 2009) and calculated the age based on the younger population. The OSL dates of the sediment are between ~0.7 and 118 ka.

Eight samples were collected for OSL dating (BY1–8) in the Ban Yod trench (**Figure 6**). The OSL ages indicated that the sediments in the trench wall were deposited since 32.2 ± 6.4 ka. Based on the stratigraphic unit and OSL ages, three earthquake events occurred at ~30, 8, and 3 ka.

Eight samples (KY1–8) were collected for OSL dating from the Khun Yuam trench (**Figure 7**). The OSL ages indicated that the sediments in the trench wall were deposited since 22.5 ± 3.8 ka and earthquakes occurred at ~30 and 3 ka.

Six samples were collected for OSL dating (MTL1–6) from the Mae Tha Lu trench (**Figure 8**). The OSL ages indicated that the sediments in the trench wall were deposited since 118 ± 43 ka and an earthquake occurred older than the oldest sediment age (unit B) at 118 ± 43 ka as the unit B deposited after the observed fault cut the unit A.

5 DISCUSSION

5.1 Paleoearthquake Events and Recurrence Interval

The alignment of geochronological data from this study and previous works (Department of Mineral Resources, 2007; Wiwegwin et al., 2014; Chansom et al., 2019) suggests that there have been nine earthquakes occurred by the MHSF. All earthquake events with dating results are described later in chronological order. It should be noted that our results are included since the fourth earthquake (**Figure 9**).

The first earthquake is related to the offset sedimentary layers on the Phra That Chom Kitti segment (**Figure 9**), as reported earlier by Wiwegwin et al. (2014). The fault cuts a sedimentary unit that was OSL and TL dated by Wiwegwin et al. (2014)to 89.7 ± 6.5 ka, and the movement must be younger than this unit. Based on the ages by Wiwegwin et al. (2014), the timing of the event is roughly constrained as having occurred at ~78 ka.

The second earthquake is intimately related to a movement on the Ban Pae segment according to Department of Mineral Resources (2007). The fault cuts through a sedimentary unit that was deposited at 69.7 ± 1.3 ka based on the OSL age (**Figure 9**; Department of Mineral Resources, 2007). Therefore, the timing of the earthquake event was reinterpreted as having occurred at ~68 ka (Wiwegwin et al., 2014).

The third earthquake is demonstrated by the movement of the Mok Chum Pae segment. The fault cuts sediment layers deposited during the period of 58.7–57.7 ka based on the OSL age of Wiwegwin et al. (2014). They interpreted the timing of the event that might have occurred at ~58 ka.

The fourth earthquake is determined by the movement on the Phra That Chom Kitti segment (Wiwegwin et al., 2014). The fault cuts the lower part of sediment layers deposited during the period of 53.3 ± 4.8 to 41.2 ± 3.5 ka (not cutting the upper part). This event was also evident on the Mae Tha Lu segment and is related to a movement of the fault cutting unit A prior to the sediment layers deposited at 26.3 ± 4.8 ka (unit B). Thus, the timing of the earthquake event might have occurred during the period of ~53.0–41.2 ka.

The fifth earthquake is evident from the offset recognized on the Doi Wiang Luang segment (Chansom et al., 2019). The fault cuts through a sedimentary unit (unit B) that was deposited at 77.3 ± 9.4 ka and cuts through units B–E. The movement must be younger than unit F which was deposited at 34.3 ± 2.4 ka. Thus, based on the OSL ages, it is possible that this fault was active at ~34.3 ka. This paleoearthquake event was also recognized in the Phra That Chom Kitti segment that was reported by Wiwegwin et al. (2014).

The sixth earthquake event is visible from the offset sedimentary layers on the Phra That Chom Kitti segments (Wiwegwin et al., 2014). The fault cuts the lower part of the sediment deposit at 27.6 ± 2.0 ka. Therefore, based on OSL age data of this study and Wiwegwin et al. (2014), it is likely that this fault might occur at ~30 ka.

The seventh earthquake is related to the offset sedimentary layers on the Mae La Noi segment and Doi Wiang Luang segment as reported by Wiwegwin et al. (2014) and Chansom et al. (2019), respectively. Based on the OSL ages of Wiwegwin et al. (2014) and Chansom et al. (2019), it is possible that this fault was active before ~22 ka.

The eighth earthquake occurred at ~8.0 ka. The event is related to the offset sedimentary layers on the Ban Yod segment, Mae La Noi segment, and Mok Chum Pae segment (Wiwegwin et al., 2014).

The last earthquake occurred at ~3.0 ka, as confirmed by our OSL dating at the Khun Yuam and Ban Yod segments. However, evidence for this youngest faulting event is clear in the trench.

From the dating of these past earthquakes, the recurrence interval of the MHSF is approximately ~5 ka (**Figure 9**). This refines the previous studies such as Wiwegwin et al. (2014) that estimated the recurrence interval of the MHSF to be ~10 ka.

5.2 Determination on Slip Rates

This study determined both lateral and vertical slip rates from the probability distribution of the displacement of the fault and the age of the earthquakes using the MATLAB code of Zechar and Frankel (2009) to calculate the slip rate and propagate the uncertainties in the displacements and age earthquakes as found in the trench. For the lateral slip rate determination, we used five offset streams at the southern terminus of the Ban Yod segment of the MHSF, with an offset of 4 ± 0.1 m and a latest earthquake event age of 3 ± 1 ka to yield a slip rate of 1.3 + 0.7/−0.3 mm/a. (**Table 3**). Four offset streams were found at the Mae Tha Lu segment with an offset of 6.6 + 3.3/−2.6 m and an OSL age of 48 ± 10 ka, yielding a slip rate of 0.1 ± 0.1 mm/a.

For the vertical slip rate, using the vertical offsets at the Khun Yuam trench is ~20 cm and the Doi Wiang Luang road cut exposure is ~75 cm and the age of a recurrence interval of the MHSF is ~5,000 year. This yields the vertical slip rates on the Khun Yuam segment and the Doi Wiang Luang segment of 0.04 and 0.15 mm/a, respectively. The average vertical offset from this study is constant with the average vertical slip rate of Wiwegwin et al. (2014) who estimated that the slip rate is ~0.03–0.13 mm/a on the Mae La Noi segment no.1 and the Phra That Chom Kitti segment. In addition, the estimated slip rate reported by

Department of Mineral Resources (2007) is ~0.0028 mm/a on the Ban Pae segment no. 31, this slip rate is less than Wiwegwin et al. (2014), and this study.

Although the MHSF is almost parallel to and has the same sense of movement as the Sagaing Fault, the slip rate of the MHSF seems to be much smaller than that of the Sagaing Fault (18 mm/a). This is on the ground that the MHSF is an inland fault that is far away from the active plate boundary whereas the Sagaing Fault represents the plate boundary between the Western Burma block and the Sibumasu block (Aung, 2005; Searle and Morley, 2011). On the other hand, the Mae Chan Fault, which lies within the complex collisional zone between the Indian and the Eurasian plates, has a slip rate of 1–2 mm/a (Weldon et al., 2016), higher than that of the MHSF. We interpreted that this is mainly due to the intraplate clockwise rotation of the mainland SE Asia block becoming larger than that of the northern part of the Shan-Thai (Sibumasu) block located more southward. The left-lateral Mae Chan Fault and other associated Nam Ma and Meng Xing faults may have accommodated and related the dextral movement of the MHSF.

5.3 Maximum Credible Earthquake

Maximum credible earthquakes (MCEs) are estimated using the fault rupture length at the surface (SRL) based on the equation proposed by Wells and Coppersmith (1994). The SRL used for the MCE calculation is the length of the longest fault segment in individual fault segments which were interpreted in Chansom (2019). The fault segments belonging to the MHSF have a wide range from 3.03 to 28.55 km. Therefore, these observations demonstrate that the dominant mode of slip across the MHSF is unstable sliding in the credible earthquakes with a maximum of Mw5.6–Mw6.8. The MCEs of the MHSF seem to be lower than those of the Mae Chan Fault–Jing Hong Fault [~Mw7.1, Xie and Tsai (1983)], and the Sagaing Fault system (~Mw 7.3; Wang et al., 2014). We consider that the MHSF consists of chopped (or broken) fault segments than those of the two fault systems. The broken geometry of the MHSF is probably large to the fault small accumulation of the slip (Wesnousky, 1988; Stirling et al., 1996; De Joussineau and Aydin, 2009). This broken fault is quite similar to the Sumatra Fault (Wang et al., 2018).

5.4 Influence of Pre-Existing Fabrics on Fault Kinematics and Basin Geometry

The MHSF is located on the boundary between the Inthanon zone and the Sibumasu block (Hisada et al., 2004), where a narrow N- trending weak zone of the Mae Sariang Trough was closed and the Inthanon zone thrust over the eastern margin of the Sibumasu block (see review in Morley, 2018). The continuous collision between the Eurasian and Indian plates during the Oligocene may have caused the reactivation of this pre-existing fabric under a N–S to NNW–SSE plate motion (Shi et al., 2018). According to ALOS DEM data, two separated N–S trending basins are present along the MHSF (**Figure 2**). Their basin geometries reflect the strong influence of the pre-existing fabrics under dextral strike-slip-dominated deformation. The MHSB is located to the north, it is ~36 km long and 7 km wide (l/w ratio = 5.16) with its lowest elevation at 180 m above the mean sea level (amsl). The basin's depocenters widen southward, separated by intrabasinal high. Many sets of offset streams and linear valleys suggest that faults within the basin are potentially tectonically active. Although Pailoplee and Charusiri (2016) suggested that large earthquakes are not likely in this region.

The Mae Sariag Basin (MSB) is located to the south with the lowest elevation at 150 m amsl. The basin is a spindle-shaped pull-apart, some 65 km long and 9 km wide (l/w ratio 7.23). The MSB represents pure strike-slip motion under a slip vector parallel to the underlapping NNW-N-trend fault segments, for example, the Mae Sariang fault splay of the Mae Ping fault zone (Smith et al., 2007), whereas the MHSB is a pull-apart basin formed under an oblique relative motion to the basin axis. The MHSB and MSB are structurally separated by Khun Yuam High (**Figure 2**) where vertical displacement decreases. There is no thoroughgoing fault formed between the two basins indicating a low amount (a few km) of dextral strike-slip displacement of the MHSF. Outcrop study along the Mae Ping fault zone suggests minor dextral deformation probably in the order of kilometers (Smith et al., 2007). Therefore, the MHSF is currently undergoing episodic, low-strain-rate dextral motion, with crustal deformation resulting in the formation of MHSB and MSB.

6 CONCLUSION

We draw the following conclusions:

1) The MHSF is mainly a right-lateral strike-slip fault trending north with some northwest and northeast direction traces and landforms along the fault including offset streams, triangular facets, shuttle ridges, linear valleys, and fault scarps.
2) The MHSF has produced at least nine earthquakes over the past ~43.0 ka in the Holocene, yielding the recurrence interval of ~5.0 ka. The maximum credible earthquake of the MHSF range from Mw 5.6 to 6.8, estimated by the surface rupture length of about ~3.0–28.5 km, which results in the slip rate of ~0.04–0.15 mm/a.
3) The MHSF has a low amount (a few km) of dextral strike-slip displacement. The north-trending MHSB and MSB in the northern and southern parts of the MHSF are structurally separated by Khun Yuam High with no geomorphic evidence of thoroughgoing large-displacement strike-slip fault segment between the basins.
4) The broader implications of this study include the low rates of slip on the MHSF and scattered small earthquakes may be common yet difficult to identify with seismologic observations. Therefore, predictions of the anomalous seismogenic behavior of MHSF are not consistent, which suggests that it is neither weak and creeping, nor does it generate anomalously large earthquakes with exceptionally long recurrence intervals. Rather, our results suggest

that the seismogenic behavior of the MHSF is very similar to other more optimally oriented faults in northern Thailand.

DATA AVAILABILITY STATEMENT

The original contributions presented in the study are included in the article/supplementary material; further inquiries can be directed to the corresponding author.

AUTHOR CONTRIBUTIONS

CC, WW, and PC contributed to the fieldwork and paleoearthquake study. CC and LO contributed to earthquake dating. SJ performed structural interpretation, basin analysis, and produced figures of the manuscript. CC, SJ, and PC wrote the first draft of the manuscript. All authors contributed to manuscript revision, read, and approved the submitted version.

FUNDING

This research was supported by the Overseas Research Experience Scholarship for Graduate Student from Graduate School, Chulalongkorn University.

ACKNOWLEDGMENTS

We are grateful to Dr. Paula M. Figueiredo and Dr. Peerasit Surakietchai who aided with OSL dating. We also thank Suwith Kosuwan and Tassana Jadeanan who aided with the trenching and discussions. We appreciated helpful comments and suggestions from an reviewer that led to improvements in this study.

REFERENCES

Adamiec, G., and Aitken, M. (1998). Dose-Rate Conversion Factors: Update. *Ancient TL* 16, 37–50.

Allen, J. R. L. (1982). "Sedimentary Structures: Their Character and Physical Basis," in *Developments in Sedimentology*. (Amsterdam: Elsevier), 593

Allen, C. R., Gillespie, A. R., Yuan, H., Sieh, K. E., Buchun, Z., and Chengnan, Z. (1984). Red River and Associated Faults, Yunnan Province, China: Quaternary Geology, Slip Rates, and Seismic Hazard. *Geol. Soc. Am. Bull.* 95, 686–700. doi:10.1130/0016-7606(1984)95<686:rraafy>2.0.co;2

Aung, T. (2005). *Dextral Shearing and Related Structural Deformation along the Sagaing Fault, between Lat 18o 15' N and 21o 15' N, Central Myanmar*. Master's Thesis. University of Yangon.

Chansom, C. (2019). Neotectonics and Paleoearthquakes along Mae Hog Son Fault, Northern Thailand. Master's thesis. Chulalongkorn University. Available at: http://cuir.car.chula.ac.th/handle/123456789/64998.

Chansom, C., Jitmahantakul, S., and Charusiri, P. (2019). "Paleoseismic Evidences of the Doi Wiang La Fault Segment, Mae Hong Son Fault, Northern of Thailand," in Proceedings of the 45th Congress on Science and Technology of Thailand, October 7–9, 2019, Chiang Rai, Thailand, 584–596.

Charusiri, P., Rhodes, B. P., Saithong, P., Kosuwan, S., Pailoplee, S., Wiwegwin, W., et al. (2007). "Regional Tectonic Setting and Seismicity of Thailand with Reference to Reservoir Construction," in International Conference on Geology of Thailand: Towards Sustainable Development and Sufficiency Economy, November 21–22, 2007, Bangkok, Thailand, 274–287.

Chen, Y., and Wu, F. T. (1989). Lancang—Gengma Earthquake: A Preliminary Report on the November 6, 1988, Event and Its Aftershocks. *Eos Trans.* 70, 1527–1540. doi:10.1029/89EO00376

DDPM (2014). Damage Reported in Several Northern Provinces after Chiang Rai Quake (In Thai). Department of Disaster Prevention and Mitigation. Available at: https://dpmcr.wordpress.com/2014/06/02/(Accessed November 6, 2019).

De Joussineau, G., and Aydin, A. (2009). The Evolution of the Damage Zone with Fault Growth and its Multiscale Characterization. *J. Geophys. Res.* 112, B12401. doi:10.1029/2006JB004711

Department of Mineral Resources (2019). *Active Faults Map in Thailand*. Technical Report. Thailand: Environmental Geology Division, Department of Mineral Resources.

Department of Mineral Resources (2007). *Investigation on Recurrence Interval in Areas Showing Trace of Movement along the Faults in the Mae Hong Son and Tak Provinces (Mae Hong Son and Mae Ping Faults)*. Technical Report. Thailand: Environmental Geology Division, Department of Mineral Resources. (in Thai).

Duncan, J.A., King, G. E., and Duller, G.A.T. (2015). DRAC: Dose Rate and Age Calculator for Trapped Charge Dating. *Quaternary Geochronology* 28, 54–61.

Durcan, J. A., King, G. E., and Duller, G. A. T. (2015). DRAC: Dose Rate and Age Calculator for Trapped Charge Dating. *Quat. Geochronol.* 28, 54–61. doi:10.1016/j.quageo.2015.03.012

Ekström, G., Nettles, M., and Dziewoński, A. M. (2012). The Global CMT Project 2004–2010: Centroid-Moment Tensors for 13,017 Earthquakes. *Phys. Earth Planet. Interiors* 200-201, 1–9. doi:10.1016/j.pepi.2012.04.002

Fenton, C. H., Charusiri, P., and Wood, S. H. (2003). Recent Paleoseismic Investigations in Northern and Western Thailand. *Ann. Geophys.* 46 (5), 957–981.

Hisada, K.-i., Sugiyama, M., Ueno, K., Charusiri, P., and Arai, S. (2004). Missing Ophiolitic Rocks along the Mae Yuam Fault as the Gondwana-Tethys Divide in North-West Thailand. *Isl. Arc* 13 (1), 119–127. doi:10.1111/j.1440-1738.2003.00412.x

Ji, L., Wang, Q., Xu, J., and Ji, C. (2017). The July 11, 1995 Myanmar-China Earthquake: A Representative Event in the Bookshelf Faulting System of Southeastern Asia Observed from JERS-1 SAR Images. *Int. J. Appl. Earth Obs. Geoinf.* 55, 43–51. doi:10.1016/j.jag.2016.10.006

Lacassin, R., Maluski, H., Leloup, P. H., Tapponnier, P., Hinthong, C., Siribhakdi, K., et al. (1997). Tertiary Diachronic Extrusion and Deformation of Western Indochina: Structural And40ar/39ar Evidence from NW Thailand. *J. Geophys. Res.* 102 (B5), 10013–10037. doi:10.1029/96jb03831

Lacassin, R., Replumaz, A., and Hervé Leloup, P. (1998). Hairpin River Loops and Slip-Sense Inversion on Southeast Asian Strike-Slip Faults. *Geology* 26 (8), 703. doi:10.1130/0091-7613(1998)026<0703:hrlass>2.3.co;2

McCaffrey, R. (2009). The Tectonic Framework of the Sumatran Subduction Zone. *Annu. Rev. Earth Planet. Sci.* 37, 345–366. doi:10.1146/annurev.earth.031208.100212

Mejdahl, V. (1979). Thermoluminescence Dating: Beta Attenuation in Quartz Grains. *Archaeometry* 21, 61–73. doi:10.1111/j.1475-4754.1979.tb00241.x

Morley, C. K. (2004). Nested Strike-Slip Duplexes, and Other Evidence for Late Cretaceous-Palaeogene Transpressional Tectonics before and during India-Eurasia Collision, in Thailand, Myanmar and Malaysia. *J. Geol. Soc.* 161 (5), 799–812. doi:10.1144/0016-764903-124

Morley, C. K. (2018). Understanding Sibumasu in the Context of Ribbon Continents. *Gondwana Res.* 64, 184–215. doi:10.1016/j.gr.2018.07.006

Morley, C. K., Smith, M., Carter, A., Charusiri, P., and Chantraprasert, S. (2007). Evolution of Deformation Styles at a Major Restraining Bend, Constraints from Cooling Histories, Mae Ping Fault Zone, Western Thailand. *Geol. Soc. Lond. Spec. Publ.* 290 (1), 325–349. doi:10.1144/sp290.12

Murray, A. S., and Wintle, A.G. (2000). Luminescence Dating of Quartz Using an Improved Single-Aliquot Regenerative-Dose Protocol. *Radiat. Meas.* 32, 57–73. doi:10.1016/S1350-4487(99)00253-X

Pailoplee, S., and Charusiri, P. (2017). Analyses of Seismic Activities and Hazards in Laos: A Seismicity Approach. *Terr. Atmos. Ocean. Sci.* 28, 843–853. doi:10.3319/tao.2017.03.23.01

Pailoplee, S., and Charusiri, P. (2016). Seismic Hazards in Thailand: A Compilation and Updated Probabilistic Analysis. *Earth Planets Space* 68, 14. doi:10.1186/s40623-016-0465-6

Pailoplee, S., Sugiyama, Y., and Charusiri, P. (2009). Deterministic and Probabilistic Seismic Hazard Analyses in Thailand and Adjacent Areas Using Active Fault Data. *Earth Planet Space* 61, 1313–1325. doi:10.1186/bf03352984

Pananont, P., Herman, M., Pornsopin, P., Furlong, K., Habangkaem, S., Waldhauser, F., et al. (2017). Seismo-Tectonics of the 2014 Chiang Rai, Thailand, Earthquake Sequence: 2014 Chiang Rai, Thailand, EQ Sequence. *J. Geophys. Res. Solid Earth* 122, 6367–6388. doi:10.1002/2017jb014085

Peltzer, G., and Tapponnier, P. (1988). Formation and Evolution of Strike-Slip Faults, Rifts, and Basins during the India-Asia Collision: An Experimental Approach. *J. Geophys. Res.* 93 (B12), 15085–15117. doi:10.1029/jb093ib12p15085

Porat, N. (2006). Use of Magnetic Separation for Purifying Quartz for Luminescence Dating. *Ancient TL* 24 (2), 33–36.

Prachaub, S. (1990). *Seismic Data and Building Code in Thailand: Technical Document No.550*. Thailand: Thai Meteorological Department, 34. (in Thai).

Prescott, J. R., and Hutton, J. T. (1994). Cosmic Ray Contributions to Dose Rates for Luminescence and ESR Dating: Large Depths and Long-Term Time Variations. *Radiat. Meas.* 23, 497–500. doi:10.1016/1350-4487(94)90086-8

Roy, S., Ghosh, U., Hazra, S., and Kayal, J. R. (2011). Fractal Dimension and B-Value Mapping in the Andaman-Sumatra Subduction Zone. *Nat. Hazards* 57, 27–37. doi:10.1007/s11069-010-9667-6

Searle, M. P., and Morley, C. K. (2011). "Tectonic and Thermal Evolution of Thailand in the Regional Context of SE Asia," in *Geology of Thailand*. Editors M. F. Ridd, A. J. Barber, and M. J. Crow (London: Geological Society), 539–571. doi:10.1144/goth.20

Shi, X., Wang, Y., Sieh, K., Weldon, R., Feng, L., Chan, C.-H., et al. (2018). Fault Slip and GPS Velocities across the Shan Plateau Define a Curved Southwestward Crustal Motion Around the Eastern Himalayan Syntaxis. *J. Geophys. Res. Solid Earth* 123, 2502–2518. doi:10.1002/2017JB015206

Smith, M., Chantraprasert, S., Morley, C., and Cartwright, I. (2007). Structural Geometry and Timing of Deformation in the Chainat Duplex, Thailand. *Geol. Soc. Spec. Publ.* 290 (1), 305–323. doi:10.1144/SP290.11

Stirling, M. W., Wesnousky, S. G., and Shimazaki, K. (1996). Fault Trace Complexity, Cumulative Slip, and the Shape of the Magnitude-Frequency Distribution for Strike-Slip Faults: A Global Survey. *Geophys. J. Int.* 124 (3), 833–868. doi:10.1111/j.1365-246x.1996.tb05641.x

Subarya, C., Chlieh, M., Prawirodirdjo, L., Avouac, J.-P., Bock, Y., Sieh, K., et al. (2006). Plate-Boundary Deformation Associated with the Great Sumatra-Andaman Earthquake. *Nature* 440, 46–51. doi:10.1038/nature04522

Thai Meteorological Department (2022). Earthquake Statistic of Thailand. (in Thai) Available at: https://earthquake.tmd.go.th/earthquakestat.html (Accessed June 4, 2022).

Tun, S. T., Wang, Y., Khaing, S. N., Thant, M., Htay, N., Htwe, Y. M. M., et al. (2014). Surface ruptures of the Mw 6.8 March 2011 Tarlay earthquake, Eastern Myanmar. *Bull. Seismol. Soc. Am.* 104 (6), 2915–2932. doi:10.1785/0120130321

USGS (2021). Earthquake Lists, Maps, and Statistics. Available at: https://www.usgs.gov/natural-hazards/earthquake-hazards/lists-maps-and-statistics (Accessed May 25, 2021).

Vermeesch, P. (2009). RadialPlotter: A Java Application for Fission Track, Luminescence and Other Radial Plots. *Radiat. Meas.* 44, 409–410. doi:10.1016/j.radmeas.2009.05.003

Wang, X., Bradley, K. E., Wei, S., and Wu, W. (2018). Active Backstop Faults in the Mentawai Region of Sumatra, Indonesia, Revealed by Teleseismic Broadband Waveform Modeling. *Earth Planet. Sci. Lett.* 483, 29–38. doi:10.1016/j.epsl.2017.11.049

Wang, Y., Sieh, K., Tun, S. T., Lai, K. Y., and Myint, T. (2014). Active Tectonics and Earthquake Potential of the Myanmar Region. *J. Geophys. Res. Solid Earth* 119, 3767–3822. doi:10.1002/2013jb010762

Weldon, E., Weldon, R., Xuhua, S., Weerachart, W., and Lewis, A. O. (2016). "The Left-Lateral Mae Chan Fault, Southern Shan Plateau, Northern Thailand: New Constraints on Slip Rate and Recency of Large Earthquakes," in Paper Presented at the Asia Oceania Geosciences Society Annual Meeting 2016, Beijing, China, July 31–August 5, 2016.

Wells, D. L., and Coppersmith, K. J. (1994). New Empirical Relationships Among Magnitude, Rupture Length, Rupture Width, Rupture Area, and Surface Displacement. *Bull. Seismol. Soc. Am.* 84 (4), 974–1002.

Wesnousky, S. G. (1988). Seismological and Structural Evolution of Strike-Slip Faults. *Nature* 335, 340–343. doi:10.1038/335340a0

Wiwegwin, W., Hisada, K.-I., Charusiri, P., Kosuwan, S., Pailopli, S., Saithong, P., et al. (2014). Paleoearthquake Investigations of the Mae Hong Son Fault, Mae Hong Son Region, Northern Thailand. *J. Earthq. Tsunami* 8 (2), 35. doi:10.1142/s1793431114500079

Wiwegwin, W., Kosuwan, S., Weldon, R., Charusiri, P., Xuhua, S., Gavillot, Y., et al. (2020). "Sip Rate and Recency of Large Paleoearthquake of Sinitral Active Faults in Indochina Region," in *The 17th World Conference on Earthquake Engineering* (17WCEE), Sendai, Japan, September 13–18, 2020.

Xie, Y. S., and Tsai, M. B. (1983). *Compilation of Historical Materials of Chinese Earthquakes*. Beijing, China: Science Press, 4912.

Zechar, J., and Frankel, K. (2009). Incorporating and Reporting Uncertainties in Fault Slip Rates. *J. Geophys. Res.* 114, 1–9. doi:10.1029/2009jb006325

Conflict of Interest: The authors declare that the research was conducted in the absence of any commercial or financial relationships that could be construed as a potential conflict of interest.

Publisher's Note: All claims expressed in this article are solely those of the authors and do not necessarily represent those of their affiliated organizations, or those of the publisher, the editors, and the reviewers. Any product that may be evaluated in this article, or claim that may be made by its manufacturer, is not guaranteed or endorsed by the publisher.